INVITED PAPERS

SPACE SHUTTLE LOADS AND DYNAMICS

SPACE SHUTTLE MAIN ENGINE (SSME) POGO TESTING AND RESULTS

J. R. Fenwick
Rockwell International, Rocketdyne Division
Canoga Park, California

and

J. H. Jones and R. E. Jewell
Marshall Space Flight Center
Huntsville, Alabama

To effectively assess the Pogo stability of the Space Shuttle vehicle, it was necessary to characterize the structural, propellant, and propulsion dynamics subsystems. Extensive analyses and comprehensive testing programs were established early in the project as an implementation of management philosophy of Pogo prevention for Space Shuttle. This paper will discuss the role of the Space Shuttle Main Engine (SSME) in the Pogo prevention plans, compare the results obtained from engine ground testing with analysis, and present measured data from STS-1 flight.

INTRODUCTION

Pogo has become one of the classical problems of structural dynamics and can be ranked along with flutter and the Tacoma Narrows Bridge as a textbook demonstration of fluid coupled structural instability. The basic Pogo loop involves resonant tuning of the vehicle structure with the propellant feed system with positive feedback through the rocket engine. The block diagram shown in Figure 1 indicates the interconnection of the major subsystems. Variations in thrust, ΔF, at the structural resonance cause large velocity variations, ΔV, which are in phase with the thrust. Tuning the propellant feedline system to the structural frequency results in engine inlet pressure oscillations, ΔP_{os}, which are in phase with velocity variations. The engine produces two effects, it acts as a blockage to the flow resulting in a downward force at the engine inlet while any fluid entering the engine is burned in the thrust chamber generating an upward thrust. Assuming negligible phase shift through the engine, it is obvious that if the downward force exerted by the pressure, P_{os}, is greater than the upward force, the net effect of the engine is that of a damper since the net engine force opposes velocity. If the upward force is the greater (the thrust), the engine acts as negative damping and for large values can become greater than the inherent damping of the structure and feed system causing divergent oscillations. In terms of the model given in Figure 1, if the first term is greater than the area, A_s, the net result is positive and this re-enforces oscillation; however if the first term is less than the area, A_s, the net result is negative and this dampens oscillations.

The second partial in Figure 1 is a measure of the engine gain; i.e. combustion chamber pressure, P_c, to engine inlet pressure, P_{os}. Consequently, with this simple model, a value of allowable engine gain for neutral or inherently stabilizing engine forces can be written as:

$$\partial Pc/\partial Ps \leq As/\frac{\partial F}{\partial Pc}$$

Allowable gain for engines used in several vehicles which displayed Pogo are shown in Figure 2. Because of the high pressure design of the SSME, an engine gain three to four times that of previous engines could be tolerated without instability. Typical engine gains are from 0.2 to 0.5 except when the engine inlet net positive suction head

(NPSH) is so low that additional gain is produced through cyclic cavitation of the turbopumps.

SIGNIFICANCE IN MANNED FLIGHT

In normal trajectories, structural modes increase in frequency while the frequency of propellant modes vary with engine inlet pressure level and tend to decrease with flight time. When tuned conditions and feedback result in an instability, divergent oscillations occur. The oscillations are a maximum when detuning results in neutral stability. Further detuning results in convergence. The envelope of an accelerometer from the second unmanned flight of Saturn V is shown in Figure 3 where closed loop damping is inferred from the envelope

Payloads are often designed to include a tolerance to Pogo when the vehicle has established a consistent amplitude and frequency over many flights. When the payload includes man, however, the only solution is to avoid Pogo. Figure 4 shows the results of vibration tests of the crew which had been chosen for the first manned Saturn V. Based on these tests and previous studies conducted during the Gemini program a limit of $\pm\frac{1}{4}G$ was established for manned flights. Since instability amplitudes are not as predictable as instability itself, the Space Shuttle Program included testing and analysis plans to prevent Pogo.

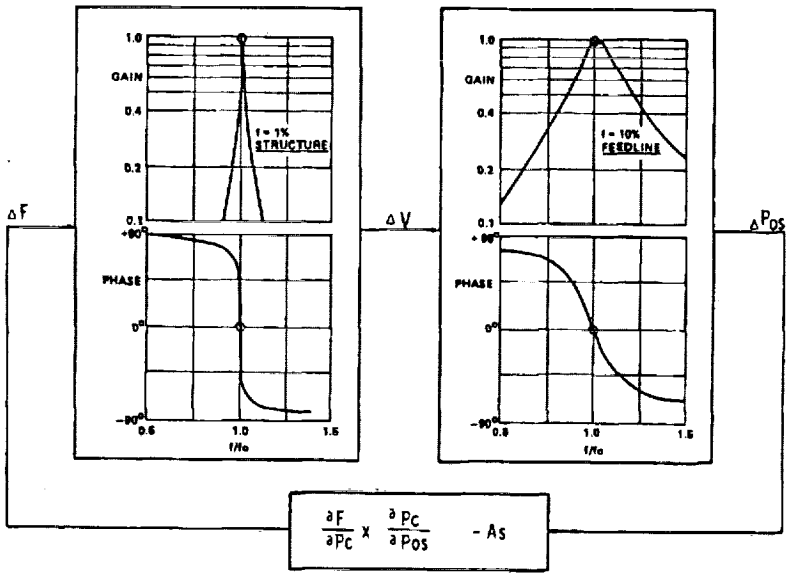

FIG. 1- POGO BLOCK DIAGRAM

VEHICLE	PROPELLANT	$As/\frac{\partial F}{\partial Pc}$
THOR	LIQUID OXYGEN	0.126
	RP-1	0.126
TITAN II	NITROGEN TETROXIDE	0.126
	HYDRAZINE/UDMH	0.087
S-IC	LIQUID OXYGEN	0.312
	RP-1	0.241
S-II	LIQUID OXYGEN	0.245
	LIQUID HYDROGEN	0.245
SPACE SHUTTLE	LIQUID OXYGEN	0.722
	LIQUID HYDROGEN	0.722

FIG. 2- COMPARISON OF $As/\frac{\partial F}{\partial Pc}$ FOR SEVERAL ENGINES INVOLVED WITH POGO

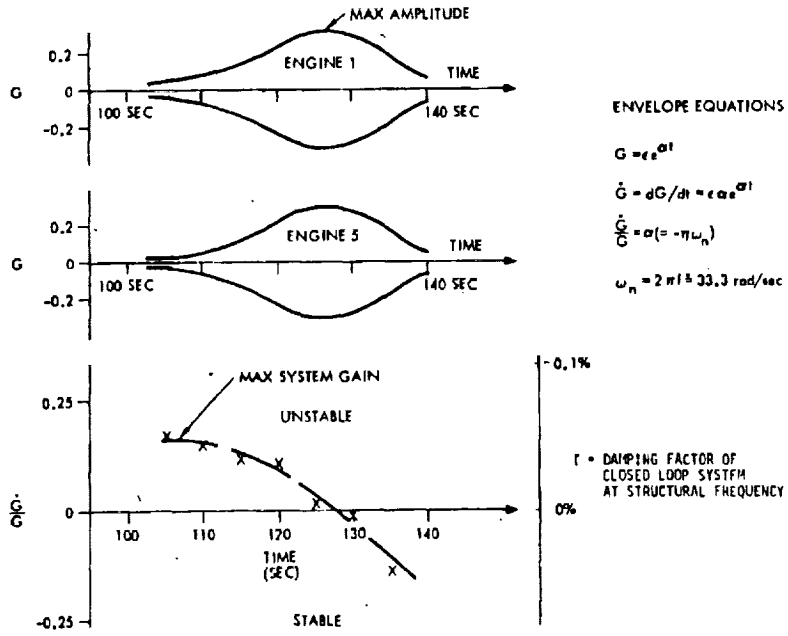

FIG.3- ENGINE GIMBAL BLOCK ACCELEROMETERS FROM APOLLO-SATURN 502 S-IC STAGE, SHOWING ENVELOPE OF OSCILLATION AND METHOD OF DETERMINING DAMPING FACTOR OF CLOSED LOOP SYSTEM AT THE STRUCTURAL MODE FREQUENCY.

ENGINE SUPPORT TO POGO PREVENTION

In the SSME (Space Shuttle Main Engine) proposal phase, dynamic testing of the engine system was included which would produce engine transfer functions of sufficient quality to allow valid vehicle stability studies. Immediately after contract awards the Pogo Integration Panel was formed and a Pogo prevention plan was formulated. It was assumed that an engine mounted Pogo suppressor would be required and, with rough estimates supplied by the vehicle contractor, Rocketdyne began generating suppressor concepts.

The Titan-Gemini vehicle propelled by storeables used a precharged nitrogen standpipe on the oxidizer system and a spring loaded piston on the fuel side. The first and second stages of the Saturn V had cryogenic propellants and the suppressor designs amounted to helium filled accumulators with a small continual gas bleed into the propellant system. Since the SSME vehicle interface is the inlet flange of the LPOTP (Low Pressure Oxygen Turbopump), an engine mounted suppressor must operate downstream of the LPOTP at a pressure level of about 500 psi with severe pressure transients at start and cutoff. Four candidate systems were chosen for further study.

SUPPRESSOR CONCEPT SELECTION

A helium charged accumulator was initially considered due to the success on Saturn V. While initial charging could be satisfied, engine cutoff would result in release of helium to the HPOTP with gross cavitation and pump overspeed. Venting and level control were not feasible. Bellows with low spring rate and structural stability could not be designed in the available volume (Figure 5). A plug valve at the suppressor throat added significant weight and operational complexity. No desirable helium system was found.

An accumulator, mounted remotely where more volume was available, was assessed. The inertia of the fluid column was so large that the frequency range and suppression capability was very limited.

As a spin-off from an LeRC (Lewis Research Center) contract, an active Pogo contract was designed. Essentially the control sensed vehicle velocity and used it to drive a piston mounted in a tee at the pump inlet as in Figure 6 and 7. As the aft end of the vehicle moves forward, the piston moved outward. Since fluid compression at the pump inlet is prevented, no significant pressure oscillations are generated due to structural

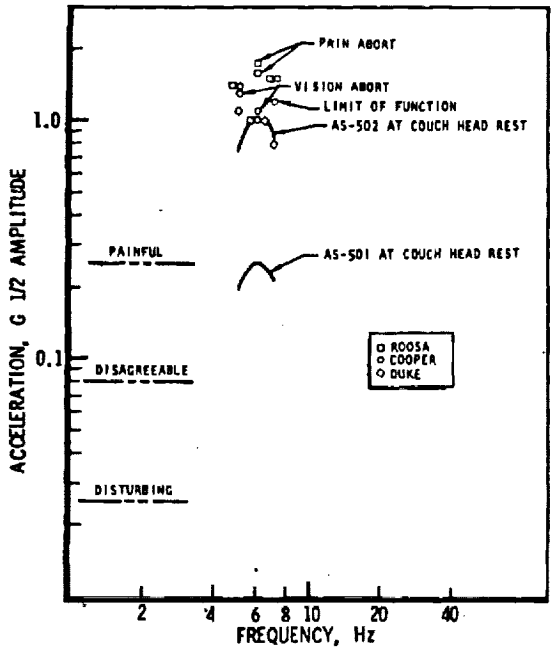

FIG. 4- COUCH VIBRATION AND AS-503 CREW ACCELERATION TOLERANCE

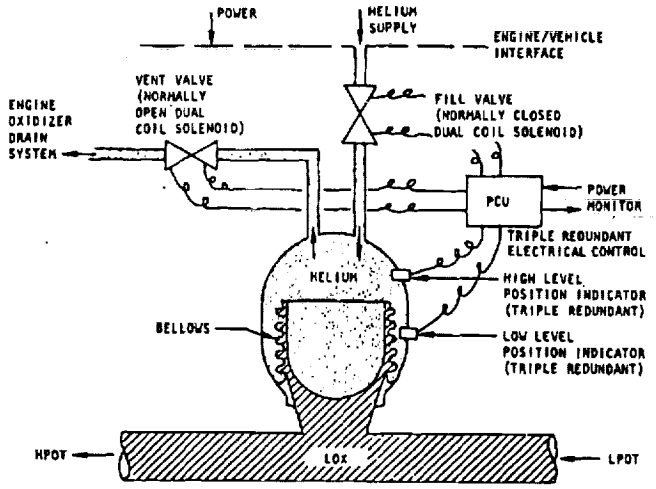

FIG. 5-BELLOWS SYSTEM SCHEMATIC

motion and the engine feedback gain is reduced. Tests and MSFC analysis indicated significant pressure attenuation in the low frequency range. The most significant problem was design of a filter to attenuate pulser motion at higher frequencies while providing less than 90% phase error through the control loop. This problem is identical to that of active dampers in large structures. While the problems of a wider bandwidth hydraulic servovalve and an adequate filter were being worked, meetings with the vehicle contractor indicated that any additional hydraulic requirement would be assessed a 1000 lb weight penalty since the hydraulics capability of the vehicle was already at its limit. The active suppressor actively was curtailed.

The fourth concept was an accumulator for the liquid oxygen system using hot gaseous oxygen. This supply was available from an engine heat exchanger which supplies pressurant for the external tank. The major potential problem was ullage stability due to heat

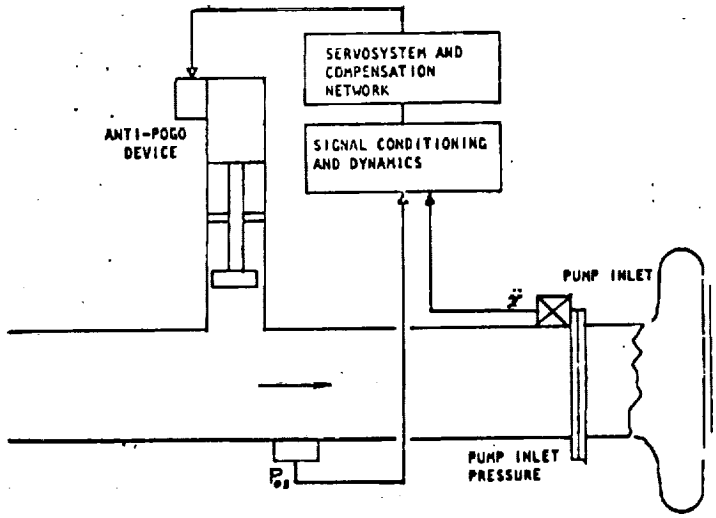

ACTIVE POGO SUPPRESSOR SCHEMATIC

FIG. 6

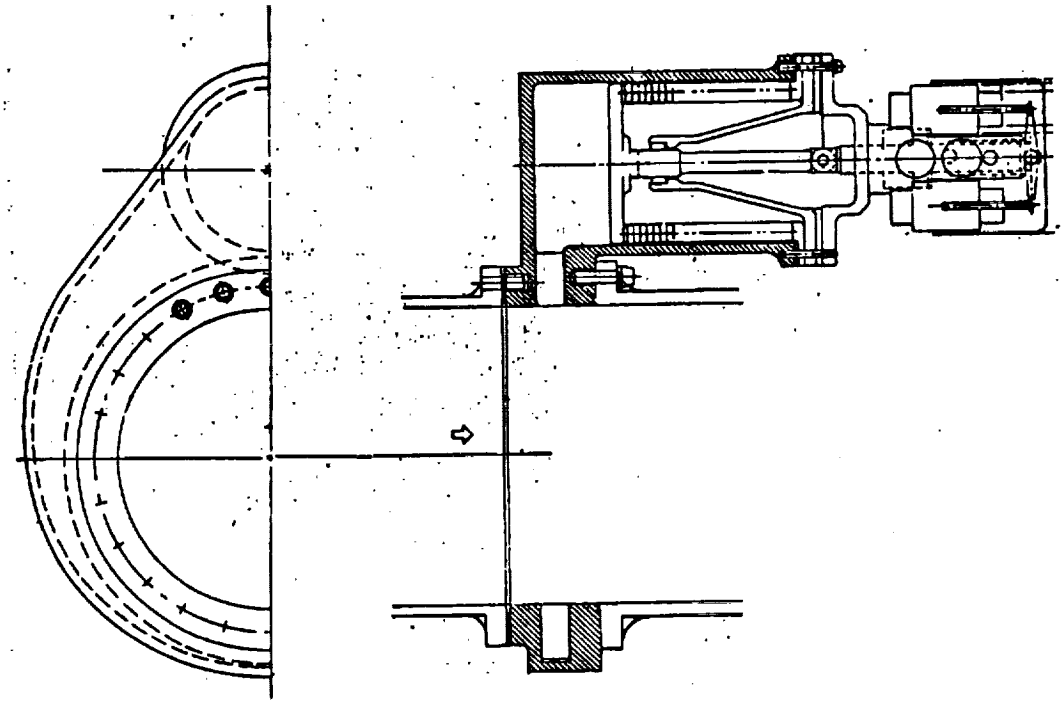

FIG. 7
CONCEPTUAL DESIGN OF FLIGHT WEIGHT POGO CONTROL

and mass transfer across the free gas-liquid interface. This problem involved the effects of sloshing, circulation of the liquid below the interface and the design of a good diffuser. The original concept is shown in Figure 8.

The suppressor systems design is shown in Figure 9. The accumulator is helium charged during engine start to about 2/3 its ullage capability. The charging valve is then shuttled to allow flow of hot oxygen gas (GOX), cutting off the helium flow. Ullage level is controlled by a tube with bleed holes at the desired interface level. The mixed gas-liquid bleed flow re-circulates into the propellant system about 15 ft. upstream of the LPOTP. At cutoff most of the gas vents through the level control. A small amount may enter the main duct but is collapsed by the flow in the main duct. Later during

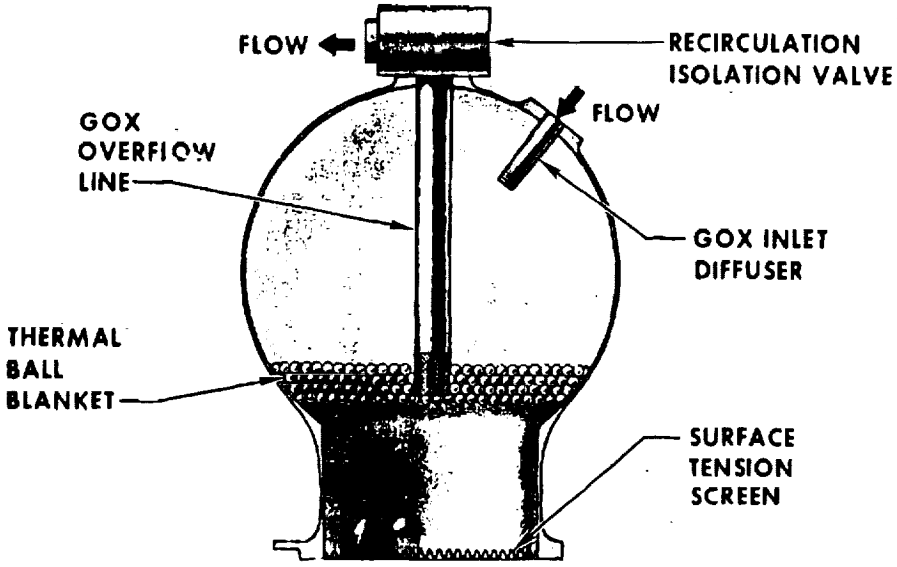

FIG. 8
POGO SUPPRESSION ACCUMULATOR

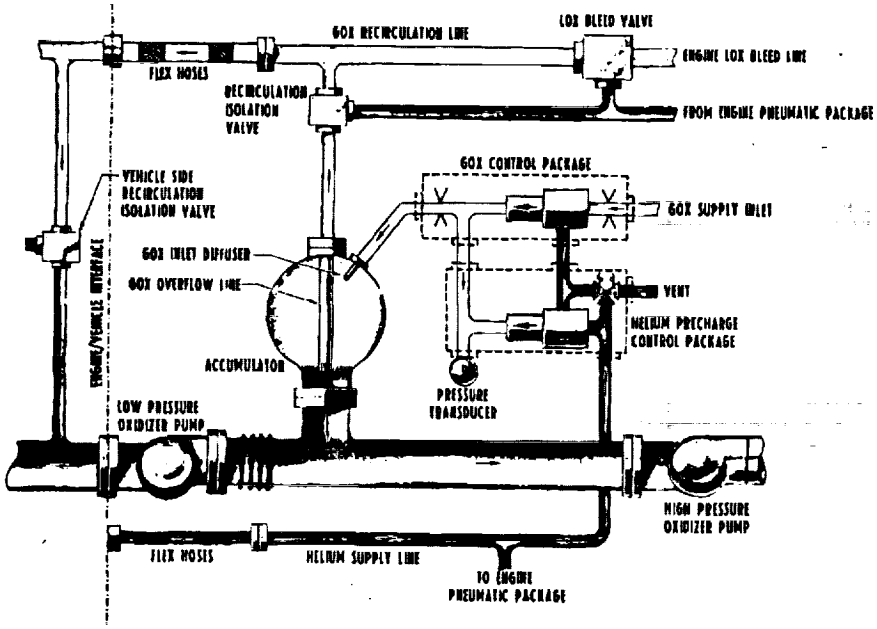

FIG. 9
POGO SUPPRESSION SYSTEM SCHEMATIC

engine testing it was found that a surge at engine cutoff could collapse the cavity sending a sharp water-hammer wave into the propellant system. A small amount of helium is now added during the cutoff sequence to eliminate the surge. This suppressor was chosen for the engine baseline primarily for its light weight (60 lb/engine) and simplicity of operation. The actual Pogo suppression system installation is shown in Figure 10.

Initial tests using low liquid flow rates and gaseous nitrogen were run to verify the level control concept and the stability of a liquid-gas interface. A plastic accumulator was also run with gaseous nitrogen and water to evaluate baffle requirements to minimize sloshing.

APPROACH TO MODEL CONSTRUCTION AND VERIFICATION

A schematic of the SSME is shown in Figure 11. The interface is at the inlet to the low pressure pumps. Frequency dependent equations representing the engines are required for the large vehicle stability models. At a minimum, transfer functions are required for the engine inlet impedance ($\Delta P_0 / \Delta \dot{M}$) and the thrust transfer function ($\Delta F / \Delta P_0$). A detailed linear model of the engine was formulated for frequency domain solution with input interfaces at both the fuel and oxidizer low pressure pump inlet flanges. A schematic of this model is contained in Figure 12

While only transfer functions connecting the interfaces are required, simpler transfer functions breaking the SSME into three subsystems were more desirable. Interfaces were chosen at the low pressure fuel and oxidizer pump inlet, the inlet to high pressure oxidizer pump and the suppressor tap-off point. The subsystems then were the LPOTP - oxidizer interpump duct, the suppressor and the powerhead. The powerhead includes the closed loop control system, preburners and thrust chamber and the complete fuel system to the vehicle-engine interface. Splitting the engine into subsystems followed the plan of subsystem testing and verification. Further, vehicle stability models are quite complicated and subsystems which can be described with low order frequency dependent polynomials are preferred to a few high order polynomials.

The initial analysis of fuel system interaction indicated that due to the low density of liquid hydrogen, the vehicle geometry and the engine mixture ratio, the contribution of the fuel system to Pogo was very small. The effect of the fuel system feedback was actually less than the predicted error band of the oxidizer system and was not required in initial analysis. These effects however were available for final vehicle verification studies.

While the engine model was quite detailed, coefficients associated with pump cavitation and suppressor dynamics could only be estimated.

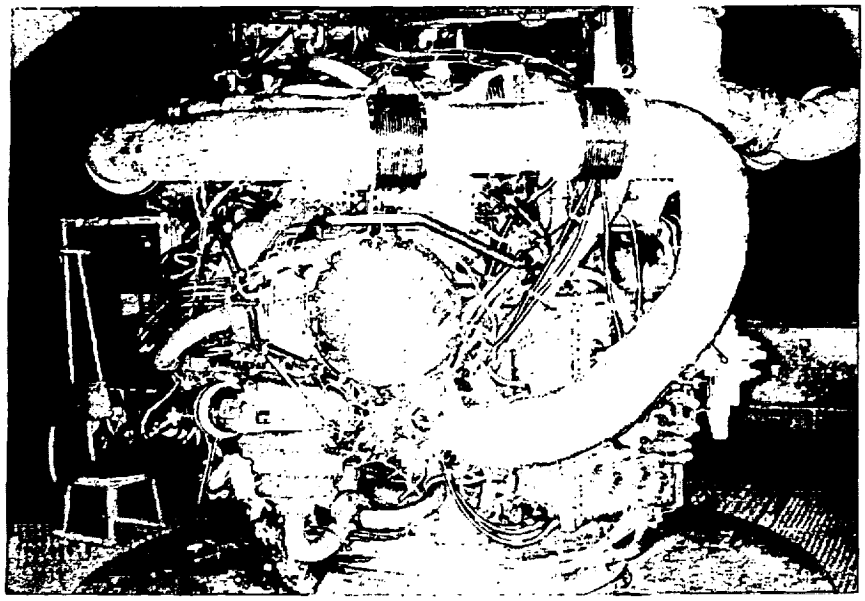

FIG. 10 - POGO SUPPRESSION SYSTEM INSTALLATION

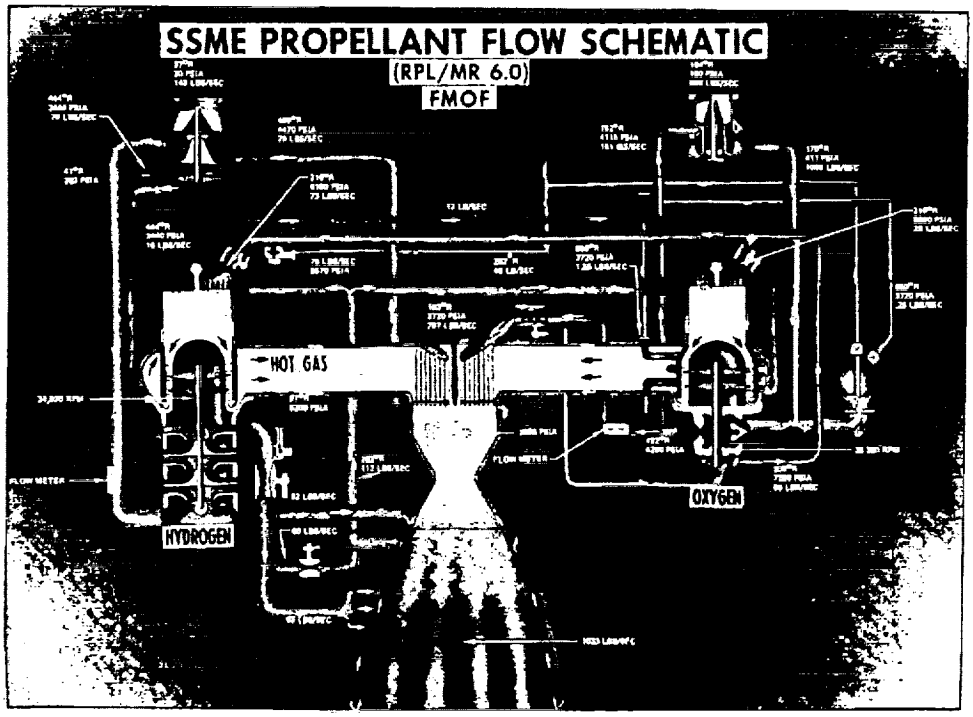

FIG. 11

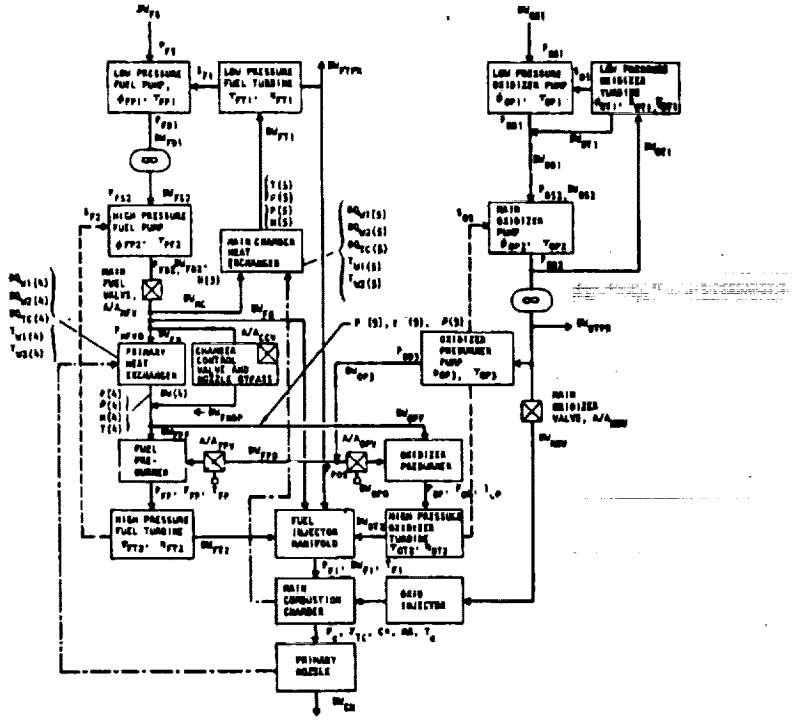

FIG. 12- SSME Flow Schematic

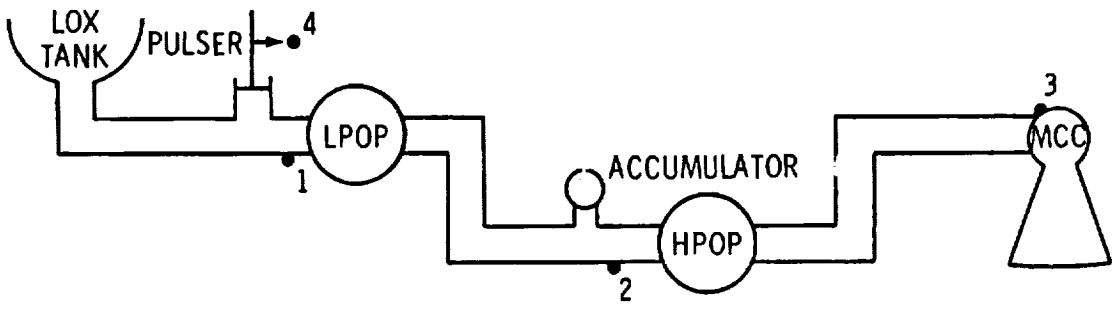

MEASUREMENT	DESCRIPTION
1	LOW PRESSURE OXIDIZER PUMP INLET PRESSURE (LPOP)
2	HIGH PRESSURE OXIDIZER TURBOPUMP INLET PRESSURE (HPOP)
3	MAIN ENGINE CHAMBER PRESSURE (MCC)
4	PULSER DISPLACEMENT

FIG. 13- GENERAL SCHEMATIC OF SSME POGO PULSING SYSTEM

The models did allow vehicle stability studies to proceed by the use of liberal tolerances on the estimated coefficients. The engine models also allowed early pre-test simulation of engine testing on the various test stands so that testing methods and hardware could be designed.

TEST METHOD DEVELOPMENT

The plan was to sinusoidally excite the oxidizer feed system over the ½ to 50 Hz range. The transmission of the disturbance would then be measured at the LPOTP inlet and outlet, HPOTP inlet and in main chamber pressure, Fig. 13. It was also planned to develop 4-terminal transfer functions for the LPOTP which could be compared with work being performed at CIT (Calif. Institute of Technology). The engine and test stand model was used to define the capability of an inlet system pulser, to provide excitation through the engine system so that instrumentation requirements could be defined and to test out data reduction methods.

Accuracy requirements for engine transfer functions were tentatively set at 10 percent on amplitude and 10 degrees on phase. To achieve this accuracy requires an even greater accuracy for the measurements used to obtain the transfer functions. A goal of 5% amplitude error and 5° phase error on any measurement relative to the excitation input was defined. This error includes the transducer, recording system, spectral analyzer and inherent signal/noise effects at the measurement point. Assuming excitation producing 10 psi P-P at the engine inlet (10% of steady state), the pressure fluctuations should be about 10 psi P-P (2% of SS) at the HPOTP inlet and about 3 psi P-P (1/10% of SS) in chamber pressure. Flow fluctuations should be about 1/10% of SS. AC coupled pressure transducers (PCB) with integral first stage amplifiers allowed a high signal level which minimized instrumentation and recording system noise. Spectral cross-correlation using the Time/Data 1932 at Rocketdyne and Hewlett Packard 5451C Fourier Analyzer at MSFC provided a very low noise method for data processing. Remaining noise inherent in the engine system became the limit for pressure measurement accuracy. That level was approximately 0.2 psi squared per Hertz.

Flow measurements to support evaluation of 4-terminal pump transfer function definition were not accomplished.

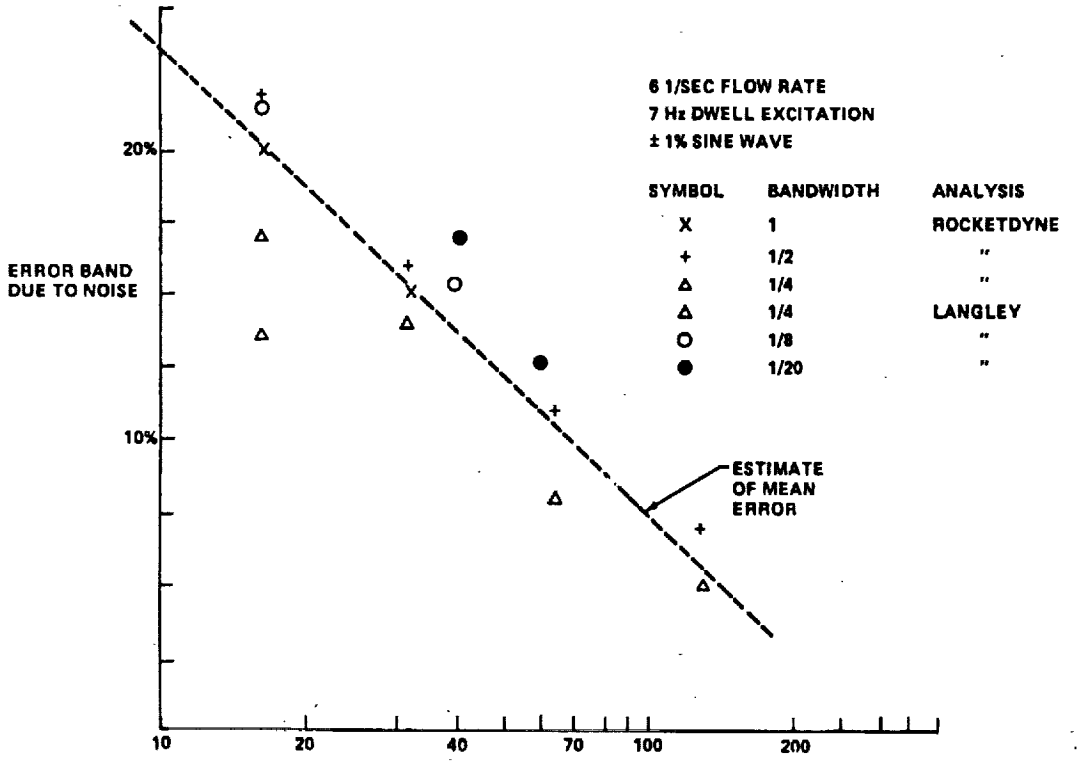

FIG. 14- LANGLEY USFM TEST
Analysis Time-Sec.

Several approaches were attempted, however, the best being a meter developed by ONERA (Office National D'Etudes Et De Researches Aerospatiales). The meter had excellent accuracy and response as shown in tests at the NASA Langley Research Center and at Rockwell's Space Systems Division. Signal/noise ratio in the actual application to Rocketdyne testing, however, showed that it was not applicable to SSME testing. A 1% flow variation at 7 Hz requires nearly 70 seconds for 10% accuracy; see Figure 14. With expected flow variations in the range of 1/10%, the engine test time required for meaningful accuracy was prohibitive. It was quite obvious that the 4-terminal pump dynamics could not be directly evaluated.

The system excitation device chosen for all transfer function testing was the hydraulic servo driven piston, pulser, shown in Figure 15. Initially the electronics were designed so that pulser position followed input voltage but studies showed that it was preferable to use a nearly constant flow rate excitation over the frequency range. The electronics were then changed so that for frequencies from 2 to 50 Hz the flow rate produced by the device was proportional to the input voltage. Later, when the device was chosen for use on the MPTA (Main Propulsion Test Article) stroke and velocity limiting circuits were added for safety. With the servo driven pulser, any excitation profile could be used. The most desirable mode of testing involved prerecording the profile on FM tape and playing it into the pulser electronics during the test. Gain of the input signal could be adjusted during a test.

Approximately 300 seconds is available for a single engine test. This is limited by the size of the propellant tanks. If one test is available to obtain transfer functions for each combination of inlet pressure and engine power level, the problem is to cover the required 2 to 40 Hz range in an efficient and safe manner.

Simulations indicated that, with constant bandwidth spectral processing, a linear frequency sweep produces uniform power across the frequency band except for transient lobes at both ends of the frequency band. Using spectral averaging techniques and starting each

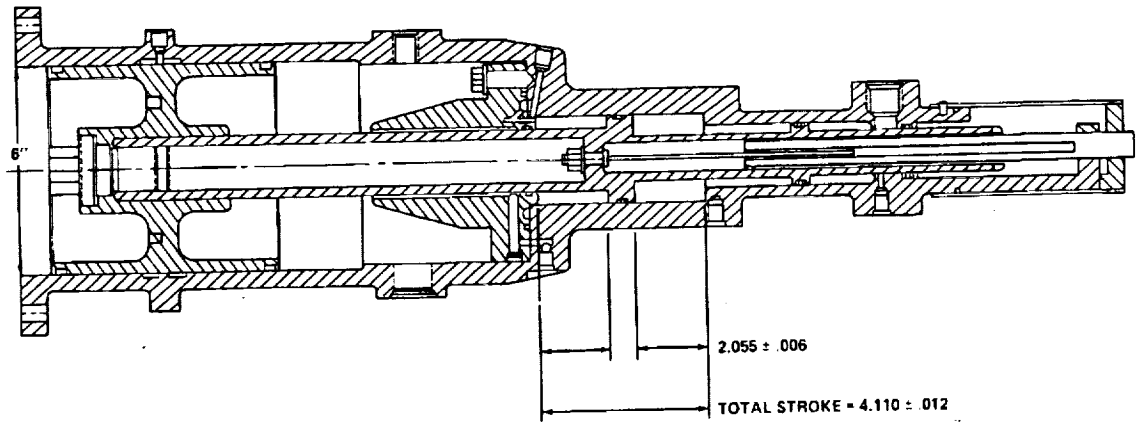

FIG. 15- SSME PULSER

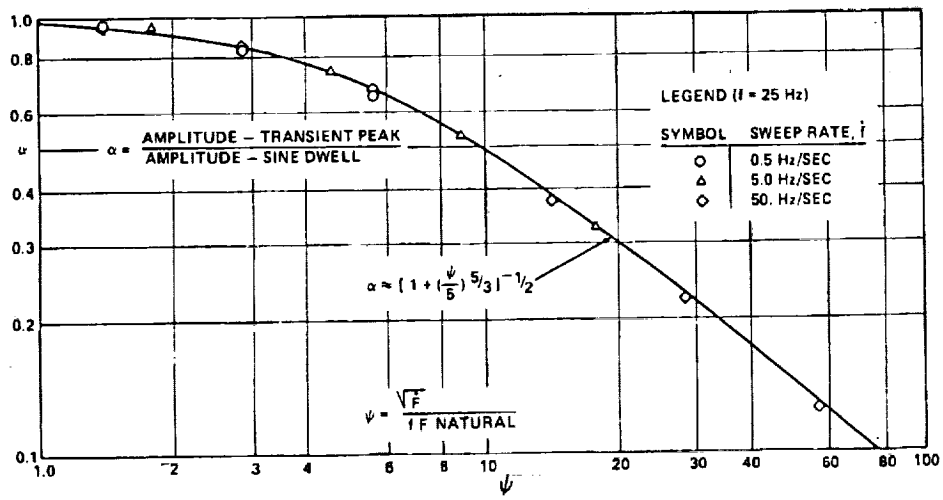

FIG. 16- TRANSIENT MAXIMUM RESPONSE FOR
SWEPT SINE EXCITATION OF A SECOND ORDER SYSTEM

sweep with a unique initial condition results in a very uniform power spectrum. While a sweep does not give the accuracy of dwell excitation at any particular frequency, it does a good job over the entire range. The effect of sweep rate was then investigated by applying the excitation to a second order system and determining the velocity response function with the Time/Data 1932. Except for systems with extremely small damping the transfer function accuracy was only a function of accumulated test time regardless of the sweep rate. It became obvious that much of the prejudice against the use of fast sweep techniques was associated with its use in very lightly damped systems and by those using tracking filter techniques rather than spectral analyzers. Figure 13 is a non-dimensional plot of the attenuation of peak velocity obtained by fast sweeping compared with the peak velocity obtained from a dwell or slow sweep test. The conclusion was that sweeps as fast as 5 to 10 sec., from 2 to 5 Hz could be used in SSME testing.

SUBSYSTEM TESTING

Component interactions in real systems obey Murphy's first law, so, to avoid program impacts, a major subsystem test facility was activated. The subsystem was composed of an LPOTP modified for electric motor drive, an interpump duct and a bread-board suppressor. The

existing facility was modified as shown in Figure 17 to anchor the inlet directly into the ground. An oil fired heat exchanger was installed to provide hot oxygen and a large decoupling accumulator was installed downstream of the test system orifice in the propellant return line (Figure 18).

The first phase of testing established the static cavitation performance of the LPOTP verifying its design goals. System testing under flow without the suppressor was next. A fast sweep profile was used and the noise problem associated with flow measurement was recognized. Initially the problem was thought to be the result of bubbles in the liquid oxygen flow stream affecting the ultrasonic beam. Even dwell pulsing did not improve the data significantly.

After the matrix of inlet pressure and simulated power level was complete the suppressor was installed. Initial checkout tests resulted in a surging condition in the system. At low helium and liquid oxygen flows the system was stable. Alternate diffuser designs and use of gaseous oxygen increased the stability range somewhat but surging still continued at flows corresponding to 50% of full power level. Tests of the plastic accumulator in a system using water and gaseous nitrogen showed the problem to be associated with high circulation in the suppressor, leading to cyclic flushing of the ullage. Several designs were tried to suppress the circulation without adding appreciable neck inertance or resistance. The Z-baffle shown in Figure 19 was chosen on the basis of best stability and performance. Tests were then run over the operational range to verify ullage stability, gaseous oxygen flow requirements and to obtain dynamic data to verify suppressor inertance and compliance.

The subsystem tests, while not providing all the information desired, were sufficient to verify the suppressor characteristics, to evaluate compliance and inertance values and to ensure compatibility with the LPOTP-interpump duct system. The strengths and weaknesses of fast sweep testing were also defined. The next step was verification of suppressor operation in single engine testing.

SINGLE ENGINE TESTING

The engine test program was being conducted on test stands A-1 and A-2 at NSTL (National Space Technology Laboratories) in Mississippi. Modifications to include a pulser tee and hydraulics as well as a level control recirculation line were made to the facilities. Initial dynamic tests showed rather lower pressure response to pulsing than had been anticipated. Ultrasonic flow meter

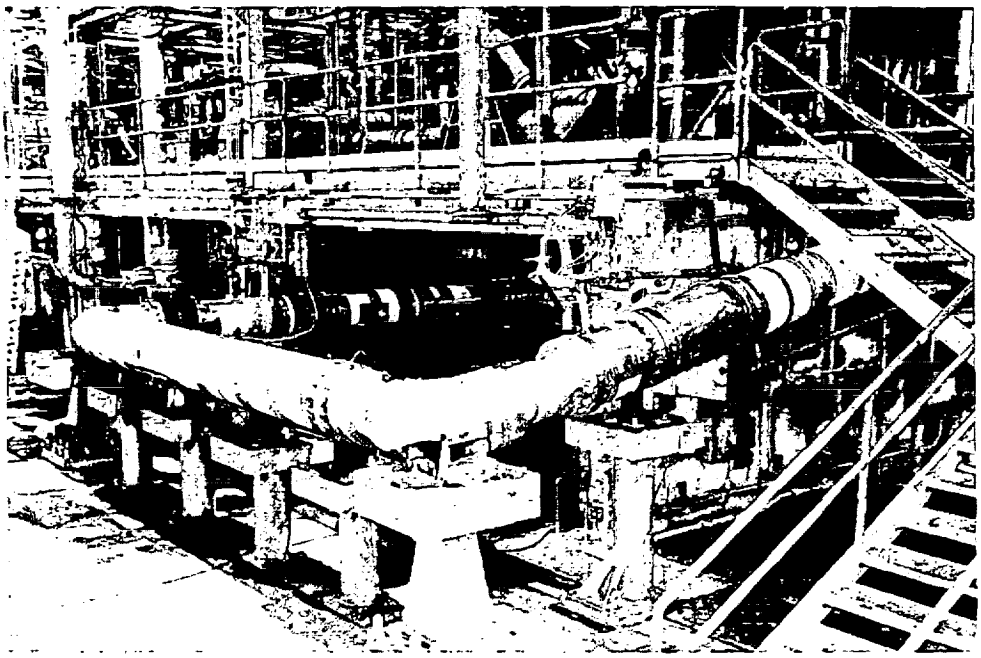

FIG. 17

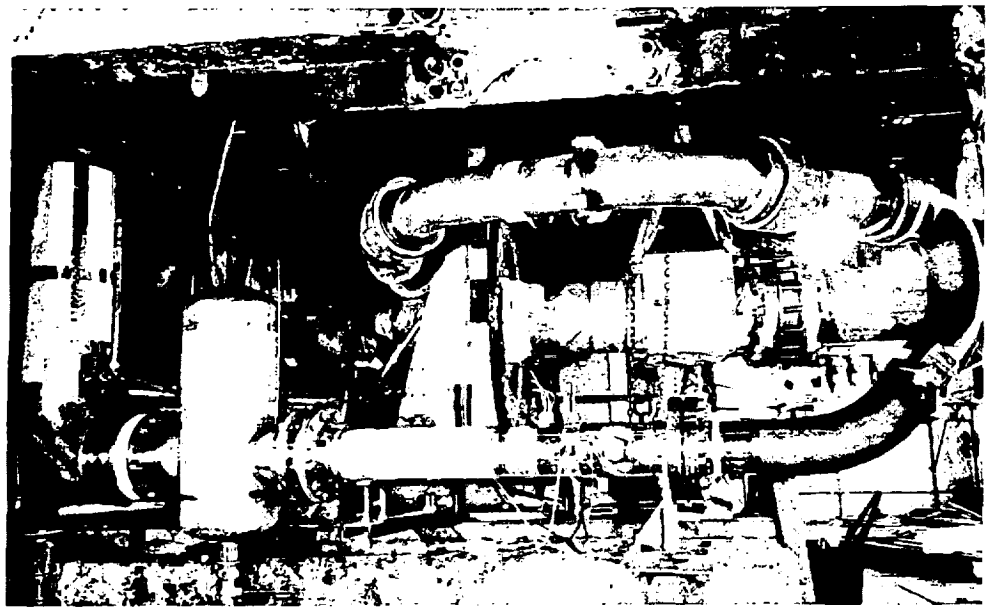

FIG. 18

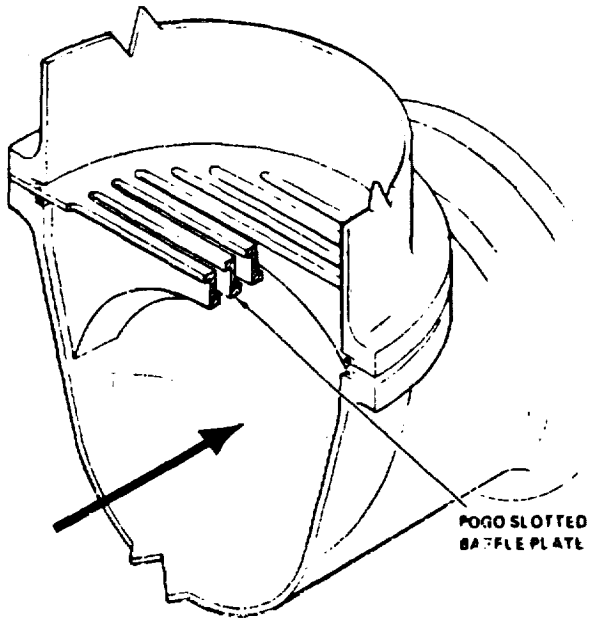

POGO Z SLOTTED BAFFLE PLATE
FIG. 19

ports which had been added earlier were utilized and again confirmed the flow noise level previously found in subsystem testing.

During static engine firings, an occasional tendency for bubble collapse at high power levels and with engine throttling transients was noted. Although the ullage re-established, an additional stage of baffling was added. These are shown in Figure 20.

Before a significant amount of dynamic testing could be accomplished, an additional test stand (A-3) was activated in Rocketdyne's Santa Susana Test Facility. At that time a program decision was made to dedicate all testing at NSTL to verification firings for the flight engines. All Pogo testing was switched to A-3.

From the minimal dynamic tests run at NSTL it was obvious that a combination of fast sweep and dwell excitation was necessary to obtain the best data over the frequency range required. The excitation profile used in this testing is shown in Figure 21. The initial 100 sec was composed of a fast sweep from 1½ to 50 to 1½ etc. with a cycle time of 15 seconds. This resulted in about six complete sweep cycles. Following this was 20 seconds at 4 Hz and 10 seconds each at 5 Hz increments to 50 Hz for a total of 110 sec of dwell. Since tests were normally about 300 seconds, the first 80 seconds were used for other test objectives i.e.; for adjusting inlet pressure and power level and for all AC coupled instruments to settle out.

The gain between the FM tape recorded reference voltage and the pulser was adjusted to ensure a safe but adequate pressure oscillation at the engine inlet. Normally this took about 2 full sweeps. Data was then obtained at a constant gain setting for the remainder of the fast sweeps and through the dwell portion.

Accelerometers installed at critical locations on the facility were initially monitored to prevent test stand damage. Note that a 12" diameter feedline pressurized to 20 psi develops a separating force of over a ton. With 1% structural damping, a ±10 psi pressure oscillation can develop equivalent static loads of over 50 tons peak to peak. Since structural resonances in the test stand did not correspond to feed system resonant frequencies where large oscillatory pressures were generated, no serious test stand loads were generated.

The most critical dynamic data collected in a test included piston input signal and pressures at the piston, the engine inlet (LPOP), the HPOTP inlet, the suppressor ullage and in the main combustion chamber pressure (see Figure 13). These data were recorded on FM magnetic tape for spectral analysis.

The test matrix was composed of engine operation at 70% and 100% power level with inlet pressures of 100 and 45 psia with and without the suppressor installed. Repeat tests were run to provide a measure of test to test differences and whenever a primary measurement was of questionable quality.

DATA ANALYSIS

Although strip charts provided a quick look for data quality, all data reduction was done using Rocketdyne's Time/Data 1932 real-time time-series analyzer and MSFC's 5451C Fourier Analyzer. Transfer functions for each pressure relative to the input pulser signal were computed using a 50 Hz low pass anti-aliasing filter and ½ Hz analysis bandwidth with a spectral band of 0 to 100 Hz.

A typical set of reduced data is shown in Figures 22 through 26 although a listing of the data was actually used to develop transfer functions for the substructured engine. Data were analyzed with spectral averaging in two independant sections, the fast sweep and dwell segments. Some of the single frequency dwell segments were analyzed separately but the minor change in data quality did not warrant this effort.

After spectral data were reduced relative to the pulser they were algebraically manipulated to obtain the substructured engine transfer functions. A special software package has been developed for use on the HP5451C (Ref. 1). This approach is shown as follows:

Let:

$F_X(f)$ → Fourier Spectrum of Input

$F_Y(f)$ → Fourier Spectrum of Output

The Transfer Function is then Defined As:

$$H_{XY}(f) = \frac{F_{XY}(f)}{F_{XX}(f)}$$

Where:

$F_{XY}(f)$ → Cross Spectrum

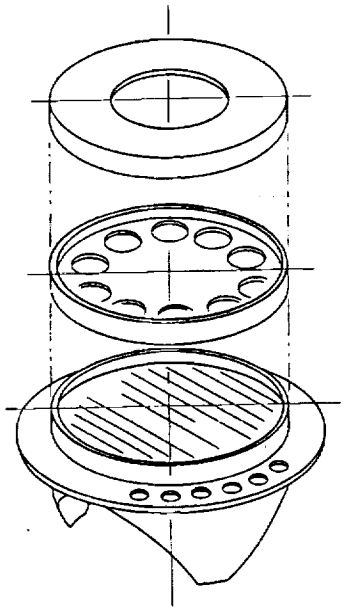

FIG. 20- POGO SPLASH PLATE

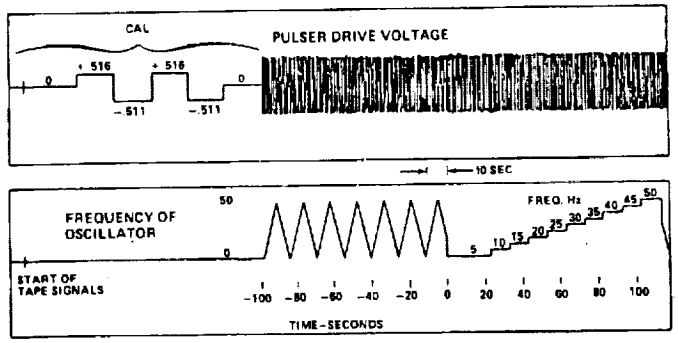

FIG. 21
POGO PULSER DRIVE TAPE FOR
SINGLE ENGINE TESTS ON A-3

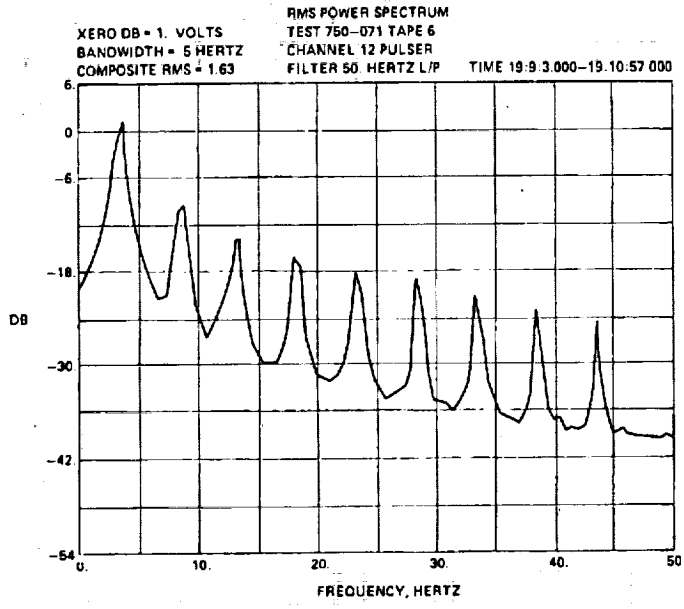

FIG. 22

$F_{XX}(f)$ Auto Spectrum

Using the concept of referencing to a common signal (the Pulser) the transfer function and coherence becomes:

$$H_{21}(f) = \frac{H_{24}(f)}{H_{14}(f)} = \frac{F_{24}(f)/F_{44}(f)}{F_{14}(f)/F_{44}(f)}$$

$HPOP_{IN}/LPOP_{IN}$

$$H_{32}(f) = \frac{H_{34}(f)}{H_{24}(f)} = \frac{F_{34}(f)/F_{44}(f)}{F_{24}(f)/F_{44}(f)}$$

$MCC/HPOP_{IN}$

$$H_{31}(f) = \frac{H_{34}(f)}{H_{14}(f)} = \frac{F_{34}(f)/F_{44}(f)}{F_{14}(f)/F_{44}(f)}$$

$MCC/LPOP_{IN}$

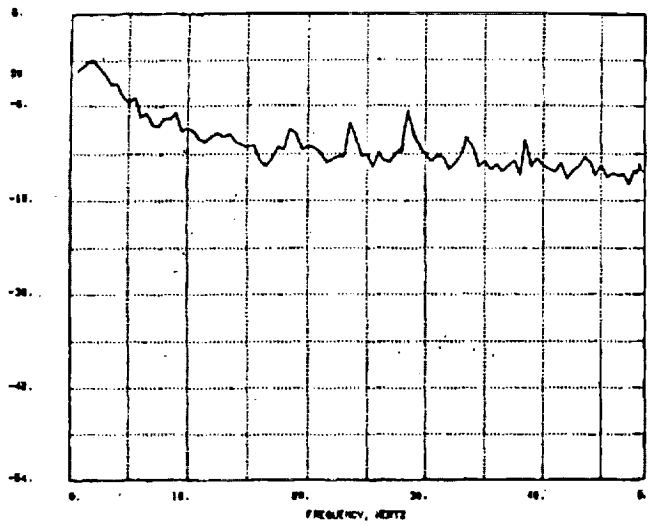

(left)
ZERO DB=1. PSI
BANDWIDTH= .5 HERTZ
COMPOSITE RMS= 3.70 PSI

RMS POWER SPECTRUM
TEST 750-071 TAPE 6
CHANNEL 11 MCC PR
FILTER 50. HERTZ L/P

FIG. 23

(right)
TRANSFER FUNCTION GAIN
TEST 750-071 TAPE 6
CHANNEL 11 MCC PR/CHANNEL
12 PULSER
FILTER 50. HERTZ L/P

ZERO DB= GAIN OF 1. PSI/VOLTS
BANDWIDTH = .5 HERTZ

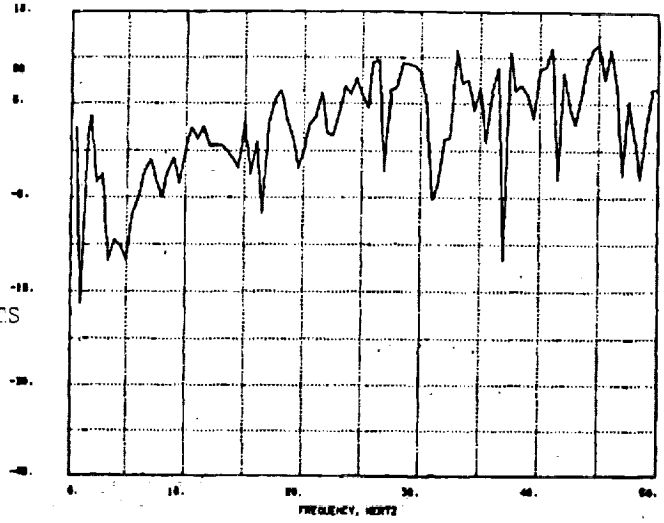

FI. 24

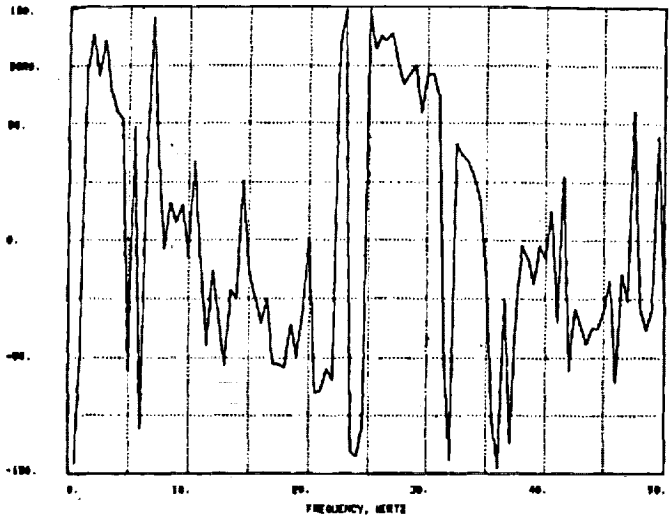

(left)
TRANSFER FUNCTION PHASE
TEST 750-071 TAPE 6
CHANNEL 11 MCC PR /CHANNEL 12 PULSER
FILTER 50. HERTZ L/P

BANDWIDTH = .5 HERTZ

FIG. 25

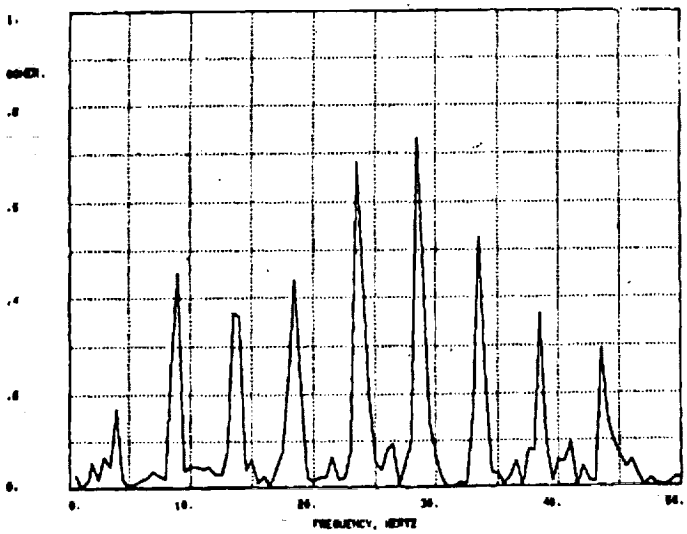

(left)
COHERENCE
TEST 750-071 TAPE 6
CHANNEL 11 MCC PR/CHANNEL 12
PULSER
FILTER 50. HERTZ L/P

BANDWIDTH = .5 HERTZ

FIG. 26

The coherence (squared) for $HPOP_{IN}/LPOP_{IN}$ is:

$$\gamma^2_{21}(f) = \left[\frac{1}{\gamma^2_{24}(f)} + \frac{1}{\gamma^2_{14}(f)} - 1 \right]^{-1}$$

The subscripts in these equations refer to the measurement numbers in Figure 13.

This approach minimized correlation of signals in the parameters which are coherent but generated in the engine itself. This engine generated noise is not associated with Pogo signals which are generated upstream of the engine and yet this engine noise shows high coherence (and erroneously high engine gain) if the pressures are correlated directly. Using the known disturbance as an intermediate reference minimizes engine generated noise effects.

INTERPRETATION OF SINGLE ENGINE TEST DATA

The two major transfer functions are the LPOTP - Interpump Duct-Suppressor $HPOP_{IN}/LPOP_{IN}$; i.e. $(\Delta P_{OS2}/\Delta P_{OS1})$ and the Power Head $MCC/HPOP_{IN}$; i.e. $(\Delta P_C/\Delta P_{OS2})$. The low pressure system transfer function changes dramatically dependent on whether the suppressor is or is not active. Figures 27 and 28 compare the test results and the original predictions.

Comparison of test data with predictions for the system with no suppressor indicated that only a very small HPOTP cavitation compliance was required to justify the model with the test data. The gain of the LPOTP-Duct is slightly less than predicted while the Power Head gain is slightly higher than predicted. Resonant dipoles were found in the LPOTP-Interpump Duct response (Figure 27) which were most readily justified with structural motion of the flexible duct.

Correlation of the model with data from tests with a suppressor installed resulted in well defined values of R, L and C for the suppressor which were within the design goals. Best of all, the suppressor is an excellent filter in the 5 to 40 Hz range with no unexpected adverse response. Gain below 4 Hz is almost unaffected by the suppressor although there is a phase effect. The suppressor effectively operates as a notch filter.

The Power Head should be defined accurately only without the suppressor since both the HPOTP inlet and main combustion chamber pressure oscillations developed by the pulser were severely attenuated by the suppressor. Thrust chamber pressure noise generated in the engine was not affected by the suppressor and the noise at the HPOTP was only slightly reduced. The net effect was a decrease in signal to noise ratio in both measurements but to a very great extent in thrust chamber pressure. A comparison of the predicted and demonstrated full engine transfer function $(MCC/LPOP_{IN})$ without suppressor is shown in Figure 29.

Extensive transfer function analysis has been performed on the SSME Pogo data obtained to date. A representative reporting of these results is given in

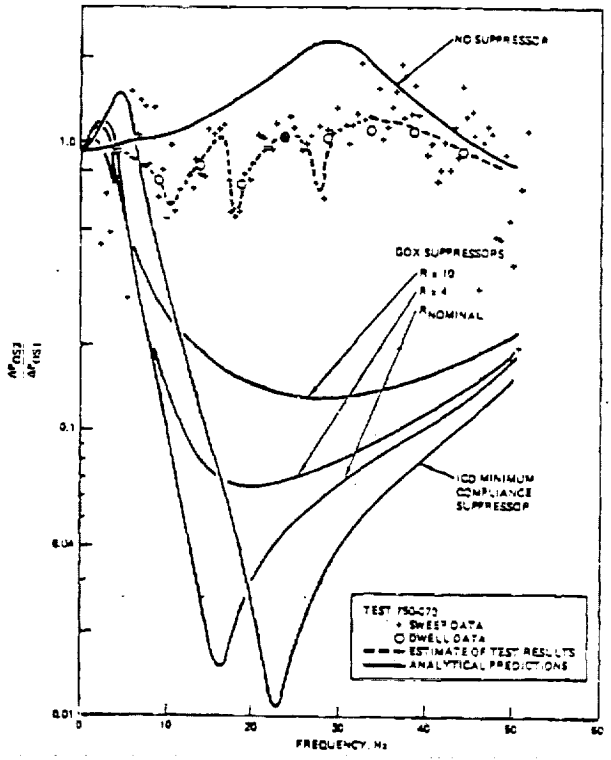

FIG. 27
Low-Pressure Oxidizer Turbopump Duct Response

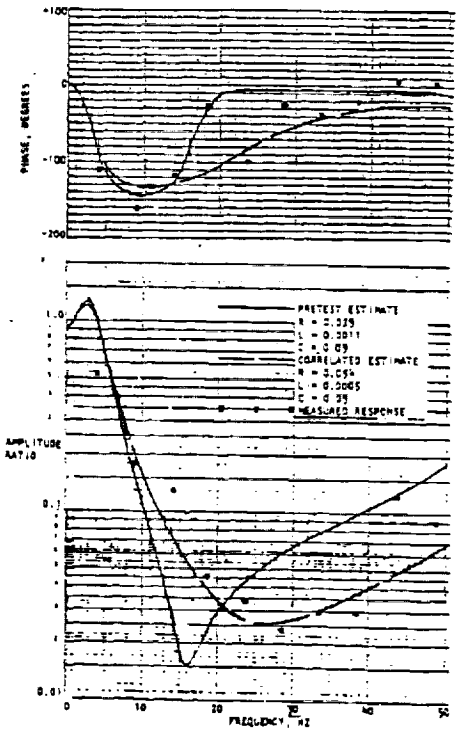

FIG. 28
HPOTP Inlet Pressure Response to Engine Oxidizer Inlet Pressure Oscillations, $\Delta P_{osz}/\Delta P_{osi}$

3 thru 6. Some test data was analyzed using a narrower spectral bandwidth (1/5 Hz). Since only 10 seconds were available for each dwell frequency, this allowed only a two sample coverage. With such a small sample the calculation indicated higher gain (due to the noise bias) and higher coherence (a single frame would show 100% coherence).

LPOTP COMPLIANCE

In parallel with the Rocketdyne testing, CIT (California Institute of Technology) conducted 4-terminal transfer function tests of a ¼ scale model of the LPOTP impeller in water. These tests included excitation both upstream and downstream of the pump over a range of inlet conditions including deep cavitation. The results of these studies are partially represented in references 7 through 21.

In actual vehicle use the inlet NPSH (net positive suction head) is higher than the critical value. This allows low risk extrapolation of the CIT results in water to the full size pump in liquid oxygen. A liberal band was placed on the extrapolated compliance values. Fortunately the feed system

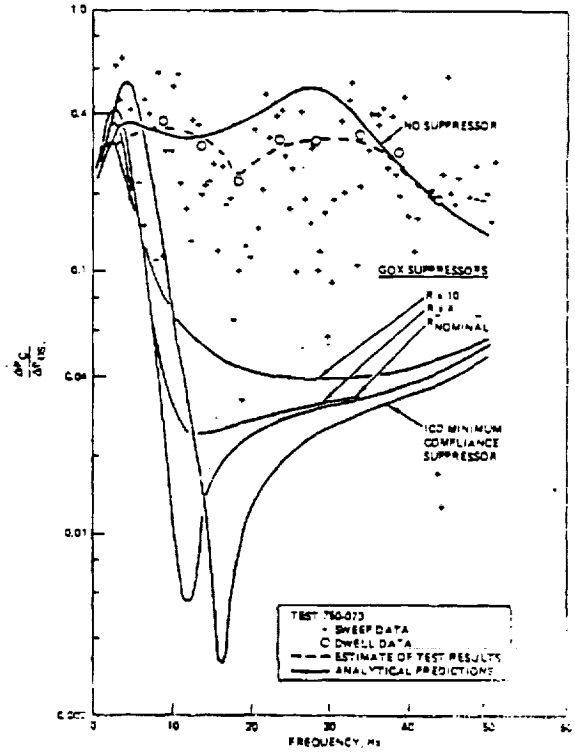

FIG. 29- ENGINE RESPONSE, CIT

dynamics are such that the changes in pump compliance cause only a small feedline frequency shift.

SUMMARY

A simple analogy of engine feedback in the Pogo loop indicates that the high pressure design of the SSME should result in the vehicle having considerably greater stability than vehicles using engines with lower internal pressure levels.

The initial analytical estimates of engine transfer functions were in good agreement with data obtained from engine and subsystem test. Over the expected operating range, cavitation affects are minor.

The suppressor design using liquid and gaseous oxygen is quite stable and an effective notch filter for the system. All the major problems of ullage stability involved circulation in the liquid below the liquid-gas interface. Design estimates of the compliance and inertance of the design were conservative although the effective resistance exceeded the initial estimate.

The use of a fast linear swept sine wave is feasible and desirable in determining transfer functions over a wide frequency band. The additional use of a few dwell excitation frequencies in the spectrum to provide accurate bench marks was also required.

The best excitation for the system involved constant velocity disturbances (flow rate perturbation) over the frequency band. The redesign of the pulses electronics to produce piston velocity proportional to command voltage eliminated input signal/noise problems in the high frequency range and allowed safety circuits to be included in the electronic package.

ACKNOWLEDGEMENTS

The work presented here is the result of the efforts of many people in many places. At Rocketdyne, the solution of difficult problems leading to the development of the two-phase suppressor was primarily due to G. H. Karigan, E. A. De Gaetano and K. C. Kan. J. G. Absalom, G. M. Smith and H. P. Yarnall were responsible for pulser development, while the electrical modifications which ensured its safe operation during testing were due to E. C. Buchanan.

At NASA MSFC, A. L. Worlund and J. E. Harbison furnished much of the early guidance in Shuttle pogo suppression. E. H. Hyde was of great support in development of both the active suppressor concept and later of the baseline suppressor. L. A. Gross contributed his own expertise in turbomachinery and was responsible for obtaining funding for Professors Brennan and Acosta leading to their timely contribution. Dr. L. Schutzenhofer and K. L. Spanyer provided estimates of the subsystem's transfer function based upon the Rocketdyne modeling equations. T. E. Nesman provided much of the transfer function analysis used at MSFC. Tony Gardner of Wyle Laboratories is recognized for his timely completion of the pogo transfer function software package.

Finally, we would like to thank J. J. Dordain and J. C. Demarais of ONERA and T. D. Carpini of NASA LaRC for their valiant effort in ultrasonic flowmeter development.

REFERENCES

1. Gardner, T. G., "Evaluation of SSME Fluid Dynamic Frequency Response Characteristics," Wyle Laboratories, Research Staff Technical Memorandum MT-80-8, Contract NAS8-33508, October 1980.

2. Jewell, R. E., "Trip Report on 24th Space Shuttle Pogo Integration Panel Meeting," NASA, MSFC, Memo ED21-80-15, June 1980.

3. Jones, J. H. and Nesman, T. E., "Single Engine SSME Pogo Data for 25th SSIP Meeting," NASA, MSFC, Memo ED24-80-33, October 1980.

4. Nesman, T. E., "Single Engine SSME Pogo Data, Quick Look," NASA, MSFC, Memorandum ED24-80-22, September 1980.

5. Nesman, T. E., "Space Shuttle Main Engine Pogo Test Results," NASA, MSFC, Memorandum ED24-80-35, November 1980.

6. Nesman, T. E., "STS-1 Pogo Analysis," NASA, MSFC, Memorandum ED24-81-31, June 1981.

7. Spanyer, K. L., "Results of Calculations from Theoretical Equations Pertaining to Pogo Transfer Functions," NASA, MSFC, Memorandum ED24-80-17, August 1980.

8. R-3128, "Final Technical Report, Thor Block 2 Test Program (20 yrs. Oscillation Problem)," Rocketdyne

Division of North American Aviation Inc., Canoga Park, CA, August 1961.

9 Prause, R. H. and Goldman, R. L., "Longitudinal Oscillation Instability Study- POGO," Martin Company, Baltimore MD, December 1964.

10 R-6929, "Engine System Transfer Functions for Support of S-V Vehicle Longitudinal Stability (POGO) Analyses Program," Rocketdyne Division of North American Aviation Inc., Canoga Park, CA, March 1967.

11 R-7970, "Investigation of 17 Hz Closed-Loop Instability on S-II Stage of Saturn V," Rocketdyne Division of North American Rockwell, Canoga Park, CA, August 1969.

12 R-7317-1, "F-1 Engine Operation in the S-IC-2 Stage of the Saturn V AS -502 Flight, Rocketdyne Division of North American Rockwell, Canoga Park, CA, September 1968.

13 Lipput, S., "Vibration Standards Proposal," SAE Journal, May 1947.

14 Saturn V Pogo Working Group, "Unpublished Briefing Charts Presented by Participating Members," NASA, MSFC, Huntsville, AL, 1968-1971.

15 RSS-8506, "Pogo-SSME Phase CD, Volume 30," Rocketdyne Division of North American Rockwell, April 1971.

16 Farrel, E. C. and Fenwick, J. R., "Pogo Instabilities Suppression Evaluation," (NASA CR-134500) Rocketdyne Division of Rockwell International, Canoga Park, CA, November 1973.

17 Fenwick, J. R., "SSME Model, Engine Dynamics Characteristics Related to Pogo," RSS-8549, Rocketdyne Division of Rockwell International, September, 1974.

18 Alais, P. and Demarais, J. C., "Measurement of Rapidly Varying Hydraulic Flow Rates by Ultrasonic Waves," (NASA Technical Translation TT F-14, 392, August 1972) originally in La Recherche Aerospatiale, No. 2, March-April 1972, pp. 61-73.

19 Brennan, C. and Acosta, A. J., "The Dynamic Transfer Functions for a Cavitating Inducer, "ASME, 75-WA/FE-16, 1975.

20 Ng, S. L., 1976, "Dynamic Response of Cavitating Turbomachines, "Ph.D Thesis, California Institute of Technology, Pasadena, CA.

21 Braisted, D. H., 1979, "Cavitation Induced Instabilities Associated With Turbomachines," Ph.D. Thesis, California Institute of Technology, Pasadena, CA.